AIChE

Counter-Intuitive Temperature Excursions During Regeneration of a Diesel Particulate Filter

K. Chen, K. S. Martirosyan, and D. Luss
Dept. of Chemical and Biomolecular Engineering, University of Houston, Houston, TX 77204

DOI 10.1002/aic.12427
Published online October 19, 2010 in Wiley Online Library (wileyonlinelibrary.com).

A major technological challenge in the regeneration of diesel particulate filters (DPFs) is that sometimes local high temperature excursions melt the cordierite ceramic filter. The cause of this melting is still an open question as the highest temperature attained under stationary (constant feed) combustion of the accumulated particulate matter is too low to cause this melting (melting temperature ~1250°C). We recently conjectured that the high temperature excursions are a counterintuitive response to a rapid deceleration, which decreases the exhaust gas temperature and flow rate and increases the oxygen concentration. Infrared measurements of the spatio-temporal temperature during soot combustion on a single-layer DPF showed that a simultaneous step change of the feed temperature, flow rate, and oxygen concentration can lead to a transient temperature that exceeds the highest attained for stationary operation under either the initial or the final operation conditions. The experiments revealed that the magnitude of the temperature rise depends in a complex way on several factors, such as the direction of movement of the propagating temperature front. The amplitude of the temperature rise is a monotonic decreasing function of the distance that the temperature front moved before the step change. The rapid response to the feed oxygen concentration increases initially the moving front temperature. The slow response of the ceramic DPF to a decrease in the feed temperature may eventually decrease the moving front temperature and even lead to premature extinction and partial regeneration. © 2010 American Institute of Chemical Engineers *AIChE J,* 57: 2229–2236, 2011
Keywords: DPF regeneration, temperature excursions, shift to idle, dynamic response

Introduction

The best existing technology for removal of particulate matter (PM) from the exhaust generated by diesel engine–driven automobiles is by a diesel particulate filter (DPF).[1] This wall-flow monolith consists of many parallel extruded square porous ceramic cells. The exhaust gases enter the inlet channels that are plugged at their end and pass through the porous walls to the four adjacent outlet channels. The PM that has accumulated in the inlet channels is periodically removed by controlled combustion, initiated by a short diesel injection to the exhaust gases.[2–4] This leads to local ignition and formation of a sharp temperature front that propagates along the surface combusting the PM.[5,6] Experience revealed that the exothermic regeneration sometimes creates excessively hot local regions that melt the cordierite ceramic filter (melting temperature ~1250°C).[7–9] Unfortunately, the knowledge and understanding of what causes the formation

Correspondence concerning this article should be addressed to D. Luss at dluss@uh.edu.

of the hot regions is still an open question. The development of a safe regeneration procedure that circumvents the local melting of the filter is the major technological challenge in the operation of DPFs.

Extensive experiments and simulations revealed that the temperature rise during stationary regeneration (fixed feed conditions) is not sufficiently high to melt the DPF ceramic support.[10–25] The chemical reaction engineering literature includes reports of counter-intuitive temperature rise during the dynamic operation of chemical reactors in which the disturbances of several state variables propagate at different velocities.[26–39] For example, there are extensive experimental and theoretical studies of the wrong-way behavior in which a rapid decrease of the feed temperature to a packed-bed or monolith reactor leads to a transient temperature exceeding the maximum obtained under stationary operation with the initial higher feed temperature.[26–39] Another counterintuitive example is the transient temperature rise following a rapid increase of the velocity of the feed to a packed-bed reactor.[40,41] This information led us to conjecture that the temperature excursions that cause the DPF melting are a dynamic response to rapid changes in the engine load. For example, a rapid change from a normal driving to idle, which increases the effluent oxygen concentration and decreases its temperature and flow rate.

Under stationary feed conditions and feed temperatures below 550°C, the PM is consumed at all points on the surface. At higher feed temperatures, the PM is combusted by a moving front. The temperature rise in either case is not sufficiently high to cause the melting of the ceramic filter. We recently started an experimental study to check the validity of the conjecture that a high temperature excursion is a dynamic response to change in the feed conditions and to determine the impact of the change in the feed on the temperature rise and the direction and velocity of the propagating temperature wave. As the combustion by a moving front leads to a higher temperature and we are interested in finding what may lead to high temperature excursions, we studied that situation. We have recently started an experimental study to check the validity of this conjecture about the dynamic temperature rise and to determine the velocity of the propagating temperature wave. We found that a step decrease of the feed temperature leads to a transient temperature exceeding the highest attained under stationary operation with the initial feed temperature. This behavior is similar to the wrong way observed in packed-bed reactors.[42] When we step changed any pair of the three state variables of the exhaust (oxygen concentration, temperature, and flow rate), the maximum transient temperature exceeded the highest temperature that could be attained under stationary operation.[43] In most cases, the maximum temperature attained during the dynamic operation was not bounded between the two limiting cases (the maximum temperature obtained at either initial or final stationary operating conditions). We report here experiments involving a simultaneous step change of the feed three state variables. This step change is similar to that caused by a rapid shift from normal driving to idle. We determined in each experiment the difference between the highest transient temperature following this step change and the highest temperature attained under stationary operation. We define this difference as the excess transient temperature rise. We also determined the highest temperature following a step change of each single feed condition and the corresponding excess transient temperature rise. These experiments enabled a comparison of the excess transient temperature rise following a step change of the three variables with the sum of the excess transient temperature rise found in the three experiments in which only one feed input was step changed. This information is of both practical value and intrinsic academic interest.

Both experiments and simulations revealed that an increase of the feed oxygen concentration or temperature increases the DPF temperature under stationary operation.[44,45] The dependence of the DPF temperature on the filtration velocity, defined as the feed flow rate divided by the surface area of the inlet channels, is more intricate. A filtration velocity increase shifts in some cases the ignition point from the upstream to the downstream. Following this shift the maximum DPF temperature is a monotonic increasing function of the filtration velocity. Eventually this trend is reversed.[46,47] All the experiments reported here were conducted under conditions that an increase in either the feed temperature, the oxygen concentration, or the filtration velocity increased the DPF temperature under stationary operation.

Experimental System and Procedure

The central part of the experimental system (Figure 1a) was a stainless steel (316 L) insulated reactor (120 mm $\times$ 40 mm $\times$ 40 mm) with an IR transparent quartz window on its top. Its temperature was controlled by an electrical heater. Inside the reactor was a planar catalytic single-layer DPF (90 mm long, 20 mm wide), cut from a commercial DPF (NGK-6000YE). Both its exterior sides and bottom were sealed by ceramic glue. Carbon black nanoparticles (40 nm, Sigma Aldridge) were deposited on top of the planar DPF by spraying a well-mixed solution of alcohol containing the nanoparticles. The alcohol was later removed by a stream of nitrogen. A schematic of the reactor is shown in Figure 1b.

To minimize the heat loss from the reactor, all sides of reactor except the one with the window were heated by an electrical ceramic fiber heater (Watlow Instruments) to a temperature set by a power controller (Staco energy product, 2PF1010). Five K-type thermocouples (diameter 0.5 mm) installed at the bottom of the single-layer DPF helped monitor its temperature during the regeneration. The first one was placed near the entrance and measured the inlet gas temperature. The second was located 10 mm downstream from the inlet; the third was located 30 mm away from the inlet, the fourth in the middle of the DPF, and the fifth 10 mm ahead of the outlet. The thermocouples' readings were recorded and processed by an Omega data acquisition board connected to a PC. A 5-mm-thick mineral wool insulation was placed between the planar DPF and the reactor walls to minimize the heat exchange with the reactor walls. The spatio-temporal temperature profile was measured by a high-speed (up to ~60 frame/s) infrared camera (Merlin, MW18, Indigo Systems) held ~50 cm above the quartz window. The camera has a 256 $\times$ 256 indium antimonide detector array sensitive to 3–5 μm radiations. Because of experimental setup limitations, we could capture images only for locations located between 30 and 90 mm from the DPF inlet. The IR

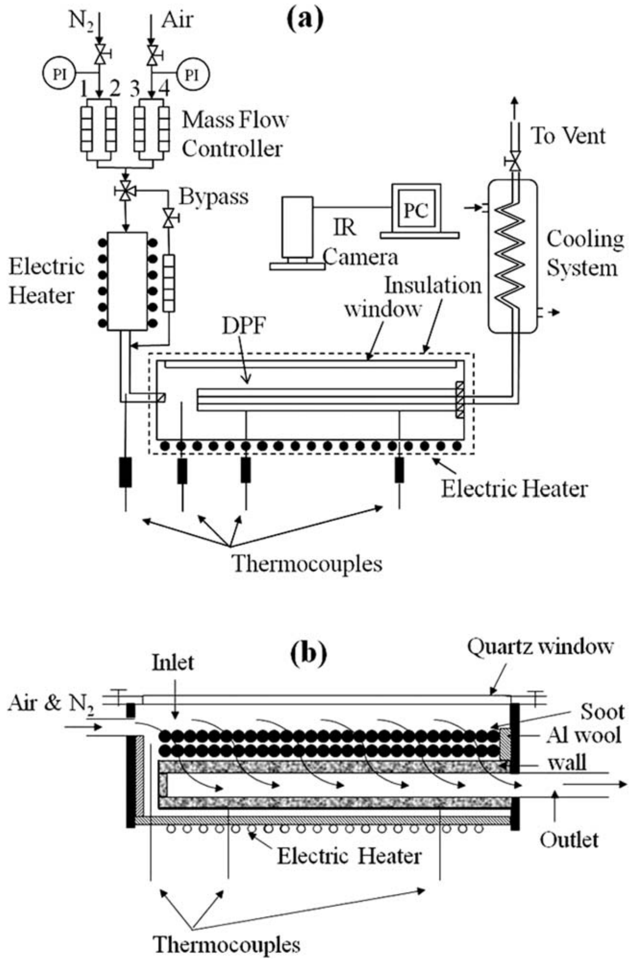

Figure 1. (a) A schematic of the experimental system; (b) a schematic of the reactor.

signals were periodically calibrated using the K-type thermocouples readings. The images were recorded at the rate of 10 s^{-1} on a PC with an ImageDesk II software.

Compressed nitrogen purged the air in the reactor before each experiment. The reactor wall temperature was then heated up from room temperature to a preset temperature. Although the reactor was fed by preheated nitrogen, the planar DPF was preheated to the desired temperature by an electric heater (Hoskins furnace, FD303). The feed pressure was controlled by downstream pressure regulators. After the DPF attained the desired temperature, a mixture of pressurized nitrogen and air was fed to the reactor. The four thermal mass flow controllers (1–4 in Figure 1a) were used to control the air/nitrogen ratio and total flow rate. The air and nitrogen flow rates were initially controlled at the desired values by two thermal mass flow controllers shown as 1 and 3 in Figure 1a (MKS, 1179A, MKS Type and ±1% accuracy). The MKS control system was used to step change the oxygen concentration and total flow rate by shifting the air and nitrogen feed to mass flow controllers 2 and 4, which were preset to the new desired values. Simultaneously, the feed temperature was lowered to the desired new value by a controlled bypass of the heater by a fraction of the gas. The step change in the feed conditions was completed within 2 s. The loaded carbon layer was usually combusted within 1 min. Each experiment was repeated at least three times to check for reproducibility.

In all the experiments described here, we measured the dynamic temperature rise caused by a sudden change of three input variables (feed temperature, oxygen concentration, and flow rate). In each case, we compared the excess transient temperature rise following a step change of the three variables with the sum of the excess transient temperature rise caused by step change of a single feed input.

Experimental Results

Experiments were conducted to determine the impact of simultaneous sudden changes of three feed conditions on the amplitude of the temporal temperature rise in comparison to the sum of the three responses to a step change of a single feed condition. We also studied the impact of the soot load and the location of the temperature front when the step change was done on the front amplitude and direction of movement. Almost all experiments reported here were conducted with a uniform soot loading of 10 g/L, which corresponded to a layer thickness of about 120 μm. The only exceptions are the experiments reported in Figures 6–8, which were conducted with a soot loading of 20 g/L. The initial feed and DPF temperature was 620°C in all experiments except the one shown in Figure 5. In all the experiments reported here, the oxygen feed concentration was 10 vol %, and the superficial filtration velocity was 12 $cm^3/(cm^2\ s)$. In all the experiments, the following simultaneous step changes were done: The oxygen concentration was increased to 15 vol %, the feed temperature decreased to

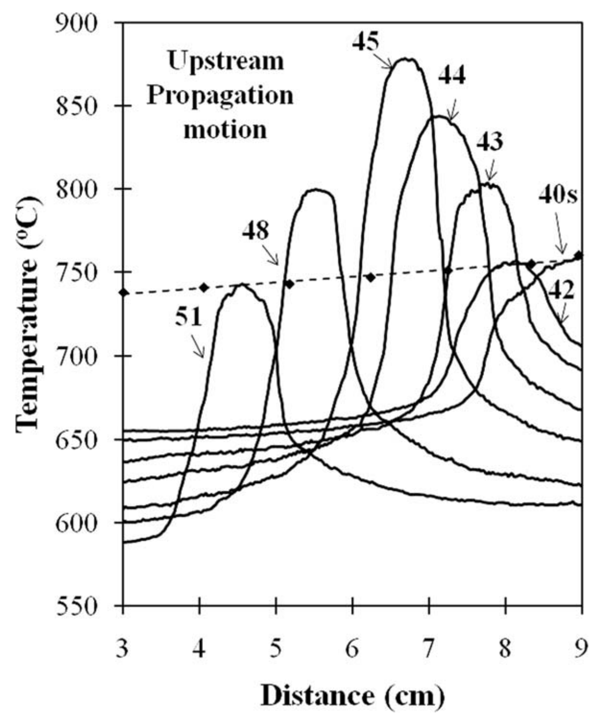

Figure 2. Response of an upstream moving front to a step change of the three feed conditions at 42 s after feed introduction to the DPF.

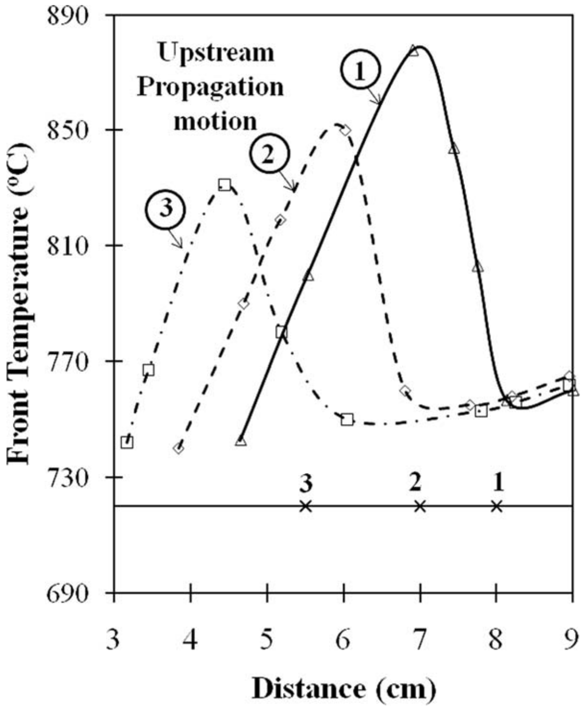

Figure 3. Moving upstream temperature profiles with the highest temperature rise following a step change of the three feed conditions in the feed at the locations marked on the horizontal line; initial feed conditions as in Figure 2.

520°C, and the filtration velocity decreased to 8.3 $cm^3/(cm^2\ s)$. The time in all the figures is that from the introduction of the reactants mixture to the reactor. The flow in all the figures is in the downstream direction, i.e., increasing distance from inlet. A dashed line with solid diamonds in all the figures is the highest local temperature under stationary initial feed conditions. In all the experiments, the step changes of either the single input or the three variables were done at the same location unless otherwise stated.

The high rate of heat removal at a high filtration velocity usually prevented ignition at the upstream of the DPF. The heat generated by the reaction in the upstream heated the downstream flowing gas, leading to a downstream ignition and formation of an upstream moving temperature front. The peak temperature decreased as this front moved upstream. Figure 2 describes such a case in which a fully developed upstream moving front formed 40 s after introduction of the hot reactive gas. Two seconds later, the three feed conditions were step changed. The sudden changes increased the temperature of the moving temperature front. The highest peak temperature of the front exceeded by 115°C that attained under stationary initial feed conditions (762°C). The decreased feed temperature eventually decreased the front peak temperature and velocity. The temperature front extinguished about 10 s after the change was implemented, so that the upstream soot was not consumed and the DPF was only partially regenerated. When stationary regeneration was conducted under the step-change conditions, a uniform and rather slow soot combustion occurred and no temperature front formed. When a step change of a single input was done at the same front position, i.e., either only the oxygen concentration increased or the temperature decreased or the filtration velocity decreased, the corresponding excess transient temperature rise was 53, 43, and 31°C, respectively. The sum of these three (127°C) was slightly higher than the 115°C when the three input variables were simultaneously step changed.

When the feed was step changed after a temperature front formed, the location of the front at that instant affected the amplitude of the peak temperature. Figure 3 describes a case in which the initial conditions led to formation of an upstream moving front, as in Figure 2. A step change of the three inputs was done when the temperature front was at a distance of 8, 7, and 5.5 cm from the DPF inlet. These positions are marked as cases 1, 2, and 3 on the horizontal line in Figure 3. The figure describes the temporal profiles with the highest temperature for each of the three cases. The peak transient temperature was a monotonic increasing function of the distance from the feed inlet when the step change was done. The excess transient temperature rise of the three cases were 115, 88, and 69°C, respectively. These are lower than the sum of the excess transient temperature rise of three single step changes (of the oxygen concentration, temperature, and filtration velocity) initiated at the same front position, which were 127, 102, and 85°C, respectively.

The experiments revealed that the soot combustion dynamics strongly depended on whether the feed step change was done either before or after the ignition and formation of a moving temperature front. Under the initial conditions used in the experiment shown in Figure 2, a temperature

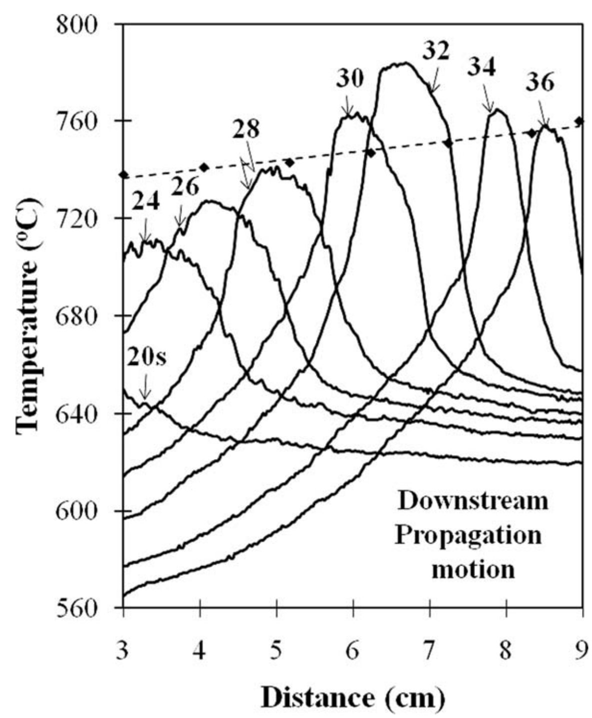

Figure 4. Response to a step change of the three feed conditions before a downstream ignition occurred 20 s after feed introduced to DPF; initial conditions as in Figure 2.

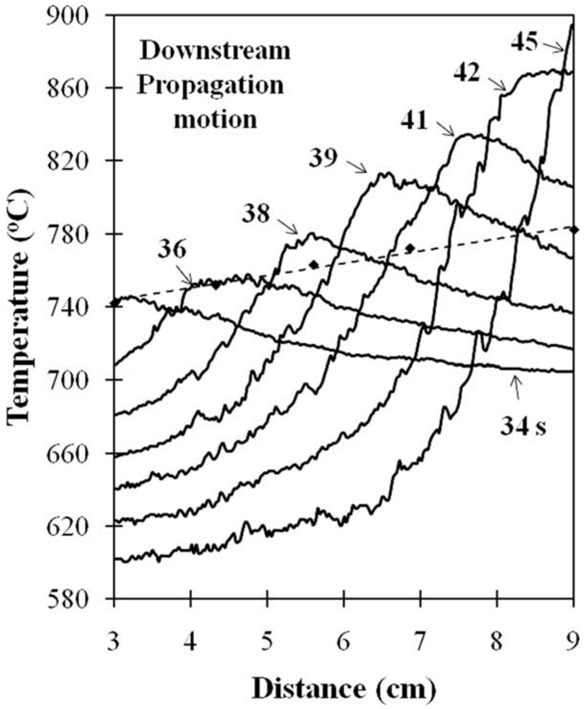

Figure 5. Response of a downstream moving front to a step change of the three feed conditions at 36 s after introduction of feed to the reactor; initial DPF and feed temperature of 650°C.

wave formed about 40 s after introducing the feed to the reactor. Figure 4 describes a case in which the step change in the three feed conditions was done 20 s after introduction of the feed, i.e., much earlier than in the case shown in Figure 2. During these 20 s, a hot zone did not form in the DPF. The step change rapidly increased the feed oxygen concentration. Although the new feed temperature was lower by 100°C from the initial one, the DPF temperature remained sufficiently high to ignite the soot because of its slow cooling due to its high heat capacity and low thermal conductivity. Ignition occurred in the upstream section of the DPF 4 s after the step change was done and a downstream moving temperature front formed. This downstream moving direction differs from the upstream direction of the moving fronts in Figures 2 and 3. The peak front temperature increased initially as it moved downstream and attained a maximum of 785°C at an axial position around 7 cm downstream from the inlet. This maximum is 23°C higher than the highest temperature of 762°C obtained under stationary operation with the initial feed conditions. The decrease in the feed temperature eventually decreased the peak moving front temperature.

The experiments revealed that at a sufficiently high temperature ignition occurred at the upstream section of the DPF, close to the inlet. This caused a rapid oxygen consumption and formation of a downstream moving temperature front. An example of such a case is shown in Figure 5. The initial feed conditions were the same as in Figure 2, but the initial feed temperature of 650°C was higher than the 620°C in Figure 2. The three feed conditions were step changed about 36 s after introduction of the feed. The peak temperature of the downstream moving front increased monotonically with their distance from the inlet. The step changes led to a peak temperature of 893°C at the end of the DPF, which exceeded by 113°C the 780°C obtained under stationary feed conditions. When stationary regeneration was conducted under the step-change conditions, no temperature front formed because of the low feed temperature, and the soot was slowly homogeneously combusted from the surface. When only a single step change was conducted at the same front location, i.e., either the oxygen concentration increased or the temperature decreased or the filtration velocity decreased, the excess transient temperature rise was 56, 45, and 25°C, respectively. The sum of these three of 126°C was slightly higher than the 113°C when the three step changes were simultaneously done.

Experience indicates that the thickness of the PM layer is not always uniform. Moreover, wall heat losses next to the DPF walls may lead to nonuniform regeneration and formation of local soot layer thicker than the surface average. The increase of the soot layer thickness increases the local oxygen consumption rate and heat generation rate and decreases the convective rate of heat removal. To determine the impact of a high local soot load, we conducted experiments with a high soot loading of 20 g/L. The initial conditions and the final step-changed conditions were the same as in Figure 2. Figure 6 shows that at beginning the ignition occurred at the upstream of the DPF forming a downstream moving front. A step change of the three feed variables 42 s after introduction of the feed generated a downstream moving front, the peak temperature of which increased as it moved downstream. The highest peak front temperature of 895°C was

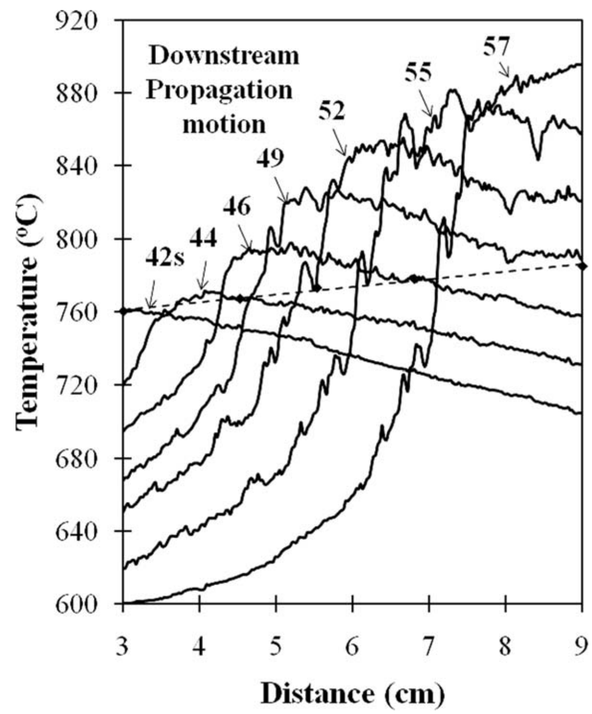

Figure 6. Response of a downstream moving front to a step change of the three feed conditions at 42 s after introduction of feed to DPF; initial soot loading of 20 g/L.

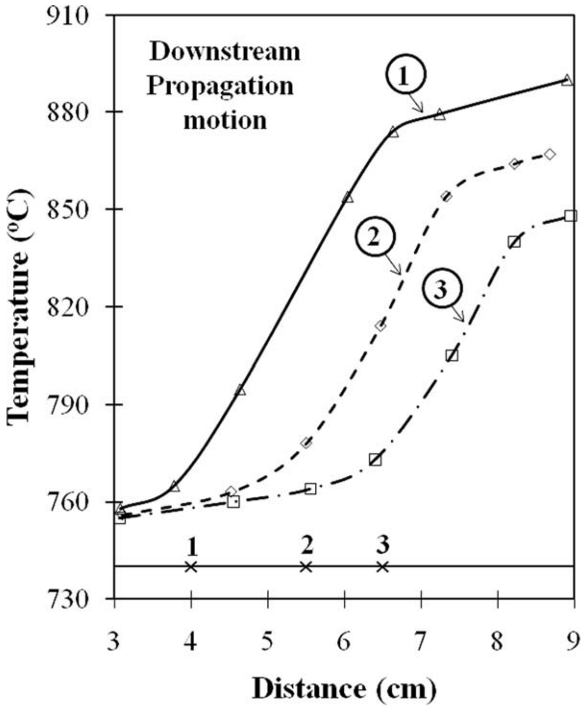

Figure 7. Moving downstream temperature profiles with the highest temperature rise following a step change in the feed at the locations marked on the horizontal line; initial soot loading of 20 g/L.

obtained at the end of the DPF. It exceeded by 122°C that under stationary operation. When only a single step change was conducted at the same front location, i.e., either the oxygen concentration increased or the temperature decreased or the filtration velocity decreased, the excess transient temperature rise was 50, 40, and 28°C, respectively. The sum of these three changes of 118°C was slightly lower than that of 122°C, when the same three step changes were done simultaneously.

When the three feed conditions were rapidly changed after a downstream moving temperature front formed, the DPF location at which the change was implemented had a strong impact on the peak transient temperature. Figure 7 shows the temporal temperature profiles with the highest temperature peak for three such cases following a feed step change when the temperature front was at a distance of 4, 5.5, and 6.5 cm from the entrance. The front positions when these three changes were done are marked on the horizontal line in Figure 7. The highest transient temperature of a downstream moving front was a monotonic decreasing function of the distance of the temperature front from the inlet when the feed step change was done. As in the upstream moving front (Figure 3), the location at which the change was done affected the amplitude of the moving front. However, it did not affect in this case its direction of motion. The temperature rise in the three cases following the step change of the three inputs was 122, 94, and 75°C, respectively. These were slightly higher than the sum of three single step changes initiated at the same front position, which were 118, 91, and 70°C, respectively.

Figure 4 shows that an early step change before a downstream ignition occurred can shift the ignition to the upstream and change the direction of the front motion. Figure 6 describes a case in which the high soot loading led to upstream ignition after 42 s. Figure 8 describes a case with the same initial conditions in which the three inputs were step changed 20 s after introduction of the feed, much earlier than the case in Figure 6. The step change rapidly increased the feed oxygen concentration. The DPF upstream section cooled much slower because of its high heat capacity and low thermal conductivity. Thus, upstream ignition occurred 5 s after the step change was done. The front peak temperature increased initially as it moved downstream and reached a maximum of 804°C at about 6 cm downstream of the inlet of the DPF. This maximum exceeds by 31°C, the highest temperature of 773°C obtained under stationary operation under the initial conditions. The decrease in the feed temperature eventually decreased the moving temperature front. This experiment showed that following an upstream ignition an early step change did not affect the location of the ignition but led to a transient increase in the moving front temperature over that obtained under stationary operation.

Discussion and Concluding Remarks

The experiments validated our conjecture that in response to a rapid change of the feed conditions to a diesel engine its temperature may exceed those obtained under stationary operation. We studied situations that are likely to produce a large excess transient temperature rise, i.e., following rapid vehicle deceleration. This step change from normal driving to

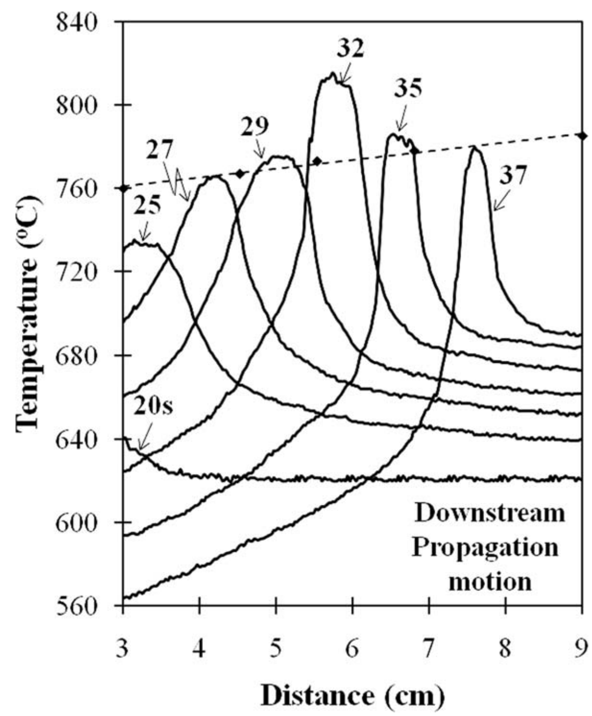

Figure 8. Response to a step change before ignition occurred 20 s after introduction of feed to DPF; initial soot loading of 20 g/L.

idle increases the feed oxygen concentration and decreases the feed temperature and filtration velocity.[3,17,48] Any increase in the oxygen concentration increases the DPF temperature. A decrease in either the feed temperature or the filtration velocity leads to a counter-intuitive temperature rise, similar to the wrong-way behavior of a packed-bed reactor.[26–36,42,43] Thus, each of these three perturbations leads to an excess transient temperature rise, i.e., increases the temperature over that under stationary operation under either the original or the final feed conditions. This counter-intuitive temperature rise may explain the unexpected reported melting of DPF, which does not happen under normal stationary operation. The experiments showed that the temperature increase due to the step change of the three inputs exceeded that generated either by a step change of any single feed condition or by a step change of any pair of feed conditions. The temperature rise caused by a step change of three inputs was rather close to the sum of temperature rise following three single changes. It will be most useful to develop design rules relating the temperature rise following several simultaneous changes to those caused by individual changes. There is a strong practical incentive and academic interest in developing simple design criteria predicting the dependence of the dynamic temperature rise on the amplitude and rate of the feed step changes. This novel understanding and know-how will be also useful for designing the control of packed-bed reactors, which are subjected to several simultaneous feed perturbations.

The experiments revealed quantitative differences in the behavior of the temperature front depending on the direction of the front motion. When the temperature front moved downstream, its peak temperature increased with distance from the inlet (Figures 5 and 6). When the front propagated upstream, the highest temperature was attained at an intermediate DPF position and it then decreased as it approached the inlet (Figure 2). The highest amplitude of either the upstream or the downstream moving front was a monotonic decreasing function of the distance that the front moved on the DPF before the step change in the feed conditions (Figures 3 and 7). We believe that these features are due to the impact of the moving front on the filtration velocity, which affects, in turn, the local temperature rise. When a temperature front moves downstream, the upstream combustion of the soot increases the filtration velocity in that section and decreases it in the downstream. When a temperature front moves upstream, the downstream combustion of the soot increases the filtration velocity in that section and decreases it in the upstream.

In all experiments, the initial DPF temperature was uniform and equal to that of the feed (either 620 or 650°C). In a regular DPF, the initial temperature is much lower than that of the heated exhaust feed. (It is usually heated by injection of diesel to the feed and its combustion in a diesel oxidation catalyst can.) Thus, an upstream ignition is much more likely to occur in a regular DPF on a car than in our experiments in which the initial DPF temperature was uniform and high. Figure 4 shows that an early step change led to an upstream ignition and a downstream propagating front even when a stationary operation under the initial conditions would have led to an upstream front propagation. The experiments showed that when the front moved downstream, which we believe is the most common behavior in a DPF, the highest temperature is attained at the downstream (Figures 5 and 6). This may explain why the damage to commercial DPFs is usually encountered in the downstream section.

The simultaneous step changes led to an initial temperature rise because of the rapid increase of the oxygen concentration at the upstream of the DPF. The response of the DPF temperature to the sudden feed temperature decrease was slower because of its high heat capacity and low thermal conductivity. Thus, although the step change initially increased the front temperature, the decrease of the feed temperature eventually decreased the front peak temperature. This led in some cases (Figure 2) to premature extinction before the front exited the DPF. This extinction can lead to a local build up of the soot on the partially regenerated areas during the next filtration cycle. A local increase in the soot film thickness decreases the local filtration velocity and convective heat removal. This may cause the regeneration temperature to exceed the highest values attained when the film thickness is uniform. The dependence of the maximum transient temperature following a step change on when it was done (Figures 3 and 7) complicates the development of simple design criteria predicting the amplitude of the transient temperature rise. It also points out the difficulty of its determining it from experiments on a commercial DPF consisting of thousands of inlet channels in which the soot layer may not be equally and uniformly deposited.

Acknowledgments

The authors thank the NSF for financial support of this research and the NGK Company for providing the DPF monolith.

Literature Cited

1. Adler J. Ceramic diesel particulate filters. *Int J Appl Ceram Technol*. 2005;2:429–439.
2. Schmidt N, Root T, Wirojsakunchai T, Schroeder E, Kolodziej C, Foster DE, Suga T, Kawai T. Detailed diesel exhaust particulate characterization and DPF regeneration behavior measurements for two different regeneration systems. Proceedings of the Society of Automotive Engineers World Congress, Detroit, MI, USA, 2007, SAE Paper No. 2007-01-1063.
3. Setten BAAL, Makkee M, Moulijn JA. Science and technology of catalytic diesel particulate filters. *Catal Rev*. 2001;43:489–564.
4. Abthoff J, Schuster HD, Langer HJ, Loose G. The regenerable trap oxidizer-an emission control technique for diesel engines. Proceedings of the Society of Automotive Engineers World Congress, Detroit, MI, USA, 1985, SAE Paper No. 850015.
5. Konstandopoulos AG, Kostoglou M, Skaperdas E, Papaioannou E, Zarvalis D, Kladopoulou E. Fundamental studies of diesel particulate filters: transient loading, regeneration and aging. Proceedings of the Society of Automotive Engineers World Congress, Detroit, MI, USA, 2000, SAE Paper No. 2000-01-1016.
6. Stratakis GA, Pontikakis GN, Stamatelos AM. Experimental validation of a fuel additive assisted regeneration model in silicon carbide diesel filters. *Proc Inst Mech Eng D*. 2004;218:729–744.
7. Cutler WA. Overview of ceramic materials for diesel particulate filter applications. *Ceram Eng Sci Proc*. 2004;25:421–430.
8. Bachiorrini A. New hypotheses on the mechanism of the deterioration of cordierite diesel filters in the presence of metal oxides. *Ceram Inst*. 1996;22:73–77.
9. Young DM, Warren CJ, Gadkaree KP, Johanessen L. Silicon carbide for diesel particulate filter applications: material development and thermal design. Proceedings of the Society of Automotive Engineers World Congress, Detroit, MI, USA, 2002, SAE Paper No. 2002-01-0324.
10. Chen K, Martirosyan KS, Luss D. Soot combustion dynamics in a planar diesel particulate filter. *Ind Eng Chem Res*. 2009;48:3323–3330.

11. Hanamura K, Suzuki T, Tanaka T, Miyairi Y. Visualization of combustion phenomena in regeneration of diesel particulate filter. Proceedings of the Society of Automotive Engineers World Congress, Detroit, MI, USA, 2003, SAE Paper No.2003-01-0836.
12. Martirosyan KS, Chen K, Luss D. Behavior features of soot combustion in diesel particulate filter. *Chem Eng Sci*. 2009;65:42–46.
13. Bissett EJ. Mathematical model of the thermal regeneration of a wall-flow monolith diesel particulate filter. *Chem Eng Sci*. 1984;39:1233–1244.
14. Bissett EJ, Shadman F. Thermal regeneration of diesel particulate monolithic filters. *AIChE J*. 1985;31:753–758.
15. Dardiotis CK, Haralampous OA, Koltsakis GC. Catalytic oxidation performance of wall-flow versus flow-through monoliths for diesel emissions control. *Ind Eng Chem Res*. 2006;45:3520–3530.
16. Haralampous OA, Koltsakis GC. Oxygen diffusion modeling in diesel particulate filter regeneration. *AIChE J*. 2004;50:2008–2019.
17. Koltsakis GC, Stamatelos AM. Modes of catalytic regeneration in diesel particulate filters. *Ind Eng Chem Res*. 1997;36:4155–4165.
18. Konstandopoulos AG, Kostoglou M, Housiada P, Vlachos N, Zarvalis D. Multichannel simulation of soot oxidation in diesel particulate filters. Proceedings of the Society of Automotive Engineers World Congress, Detroit, MI, USA, 2003, SAE Technical Paper No. 2003-01-0839.
19. Miyairi Y, Miwa S, Abe F, Xu Z, Nakasuji Y. Numerical study on forced regeneration of wall-flow diesel particulate filters. Proceedings of the Society of Automotive Engineers World Congress, Detroit, MI, USA, 2001, SAE Technical Paper No. 2001-01-0912.
20. Guo ZH, Zhang ZY. Hybrid modeling and simulation of multidimensional processes for diesel particulate filter during loading and regeneration. *Numer Heat Transfer A*. 2007;51:519–539.
21. Bensaid S, Marchisio DL, Fino D. Numerical simulation of soot filtration and combustion within diesel particulate filter. *Chem Eng Sci*. 2010;65:357–363.
22. Schejbal M, Marek M, Kubicek M, Koci P. Modeling of diesel filter for particulate removal. *Chem Eng J*. 2009;154:219–230.
23. Aoki H, Asano A, Kurazono K, Kobashi K, Sami H. Numerical simulation model for the regeneration of process of a wall-flow monolith diesel particulate filter. Proceedings of the Society of Automotive Engineers World Congress, Detroit, MI, USA, 1993, SAE Technical Paper No. 930364.
24. Opris CN, Johnson JH. A 2-D computational model describing the heat transfer, reaction kinetics and regeneration characteristics of a ceramic diesel particulate trap. Proceedings of the Society of Automotive Engineers World Congress, Detroit, MI, USA, 1998, SAE Technical Paper No. 980546.
25. Frey M, Wenninger G, Krutzsch B, Koltsakis GC, Haralampous OA, Samaras ZC. 2D simulation of the regeneration performance of a catalyzed DPF for heavy-duty applications. *Top Catal*. 2007;42/43:237–245.
26. Boreskov GK, Slinko MG. Modeling of chemical reactors. *Pure Appl Chem*. 1965;10:611–624.
27. Crider JE, Foss AS. Computational studies of transients in packed tubular chemical reactors. *AIChE J*. 1966;12:514–522.
28. Hoiberg JA, Lyche BC, Foss AS. Experimental evaluation of dynamic models for a fixed-bed catalytic reactor. *AIChE J*. 1971;17:1434–1447.
29. Mehta PS, Sams WN, Luss D. Wrong-way behavior of packed-bed reactors. I. The pseudo-homogeneous model. *AIChE J*. 1981;27:234–246.
30. Pinjala V, Chen YC, Luss D. Wrong-way behavior of packed-bed reactors. II. Impact of thermal dispersion. *AIChE J*. 1988;34:1663–1672.
31. Sharma CS, Hughes R. The behavior of an adiabatic fixed bed reactor for the oxidation of carbon monoxide. II. Effect of perturbations. *Chem Eng Sci*. 1979;34:625–634.
32. Van Doesburg H, DeJong WA. Transient behavior of an adiabatic fixed-bed methanator. I. Experiments with binary feeds of CO or CO_2 in hydrogen. *Chem Eng Sci*. 1976;31:45–51.
33. Van Doesburg H, DeJong WA. Transient behavior of an adiabatic fixed-bed methanator. II. Methanation of mixtures of carbon monoxide and carbon dioxide. *Chem Eng Sci*. 1976;31:53–58.
34. Oh SH, Cavendish JC. Transient of monolithic catalytic convertors: response to step changes in feedstream temperature as related to controlling automobile emissions. *IEC Proc Des Dev*. 1982;21:29–37.
35. Chen YC, Luss D. Wrong-way behavior of packed-bed reactors: influence of interphase transport. *AIChE J*. 1989;35:1148–1156.
36. Luss D. Temperature fronts and patterns in catalytic systems. *Ind Eng Chem Res*. 1997;36:2931–2944.
37. Dudukovic MP, Kulkami MS. Dynamics of gas phase and solid phase reactions in fixed bed reactors. *Chem Eng Sci*. 1996;51:3083–3088.
38. Sun M, Croiset EB, Hudgins RR, Silveston PL. Steady-state multiplicity and superadiabatic extinction waves in the oxidation of CO/H_2 mixtures over a Pt/Al_2O_3-coated monolith. *Ind Eng Chem Res*. 2003;42:37–45.
39. Silveston P, Hudgins RS, Renken A. Periodic operation of catalytic reactors—introduction and overview. *Catal Today*. 1995;25:91–112.
40. Ilin A, Luss D. Wrong-way behavior of packed-bed reactors: influence of reactant adsorption on support. *AIChE J*. 1992;38:1609–1617.
41. Yakhnin V, Menzinger M. High-temperature transients in catalytic fixed-bed reactors. *Rev Chem Eng*. 2004;20:175–225.
42. Chen K, Martirosyan KS, Luss D. Wrong-way behavior of soot combustion in a planar diesel particulate filter. *Ind Eng Chem Res*. 2009;48:8451–8456.
43. Chen K, Martirosyan KS, Luss D. Temperature excursions during soot regeneration in the diesel particulate filter (DPF). *Ind Eng Chem Res*. In press; doi:10.1021/ie1004465.
44. Zheng H, Keith JM. New design for efficient diesel particulate trap regeneration. *AIChE J*. 2004;50:184–191.
45. Zheng H, Keith JM. Ignition analysis of wall-flow monolith diesel particulate filters. *Catal Today*. 2004;98:113–122.
46. McCabe RW, Sinkevitch RM. A laboratory combustion study of diesel particulates containing metal additives. Proceedings of the Society of Automotive Engineers World Congress, Detroit, MI, USA, 1986, SAE Paper No. 860011.
47. Herz RK, Sinkevitch RM. Reactors for investigation of soot combustion on filter surfaces. *Carbon*. 1986;4:457–462.
48. Haralampous OA, Koltsakis GC, Samaras ZC, Kraemer L, Heimlich F, Behnk K. Control strategies for peak temperature limitation in DPF regeneration supported by validated modeling. Proceedings of the Society of Automotive Engineers World Congress, Detroit, MI, USA, 2007, SAE Technical Paper No. 2007-01-1127.

Manuscript received July 10, 2010, and revision received Aug. 25, 2010.